Journal of The
Electrochemical Society

The Aqueous Chemistry of Zirconium as a Basis for Better Understanding the Formation of Zirconium Conversion Coatings: Updated Thermodynamic Data

To cite this article: Ana Kraš and Ingrid Milošev 2023 *J. Electrochem. Soc.* **170** 021508

Journal of The Electrochemical Society, 2023 **170** 021508

The Aqueous Chemistry of Zirconium as a Basis for Better Understanding the Formation of Zirconium Conversion Coatings: Updated Thermodynamic Data

Ana Kraš[1,2] **and Ingrid Milošev**[1,z,*]

[1]*Jožef Stefan Institute, Department of Physical and Organic Chemistry, SI–1000 Ljubljana, Slovenia*
[2]*Jožef Stefan International Postgraduate School, SI–1000 Ljubljana, Slovenia*

This work tackles the aqueous chemistry of Zr, aiming to contribute to a better understanding of Zr conversion coatings as one of the important contemporary means of corrosion protection. Equilibrium predominance diagrams based on experimentally confirmed Zr–OH and Zr–F aqueous species concerning Zr amorphous solid phase, along with an updated Zr E−pH (Pourbaix) diagram, are constructed. Since ZrO^{2+} existence had been conclusively disproven in both the aqueous and solid states, we chose to depict mononuclear species with $ZrOH^{3+}$ and polynuclear with $Zr_4(OH)_8{}^{8+}$. The formation of the Zr solid phase is assumed to include Zr tetrameric species, $Zr_4(OH)_8{}^{8+}$, as a fundamental building block thereof. The role of F^- and $ZrF_6{}^{2-}$ ions in Zr conversion baths and subsequently formed coatings is described. The introduction of $ZrF_6{}^{2-}$ anions keeps Zr solvated in the form of a complex, thus preventing the early onset of hydrolysis. The conversion of Zr species and the coating formation mechanism are further discussed from electrochemical and sol-gel perspectives, aiming to give a foundation for future predictions and rationalisation of Zr conversion coating formation, with the possibility of extensions to various bath additives.
 [DOI: 10.1149/1945-7111/acb9c2]

Manuscript submitted November 22, 2022; revised manuscript received February 6, 2023. Published February 16, 2023. *This paper is part of the JES Focus Issue on Critical Factors in Localized Corrosion in Honor of Gerald Frankel.*

Supplementary material for this article is available online

Zirconium has many uses, including nuclear reactors (Zircaloy), artificial gemstones, ceramics, and cosmetics, to name a few.[1] Hence, understanding the aqueous chemistry of Zr is not only of fundamental but also practical importance. In terms of the development of corrosion–resistant coatings, zirconium conversion coatings (ZrCCs) have drawn increasing attention over the last few decades as a replacement candidate for chromate (CCCs) and phosphate conversion coatings (PCCs).[2] A comprehensive review of ZrCCs from a corrosion protection standpoint was published recently.[2]

ZrCCs are formed by pH-driven precipitation, most commonly from baths containing hexafluorozirconic acid (H_2ZrF_6). ZrCC formation can be generally expressed with reaction (1) [2]:

$$ZrF_{6\,(aq)}^{2-} + 4OH^- \rightarrow ZrO_2{\cdot}2H_2O_{(s)} + 6F^- \qquad [1]$$

Beside H_2ZrF_6, current commercial baths contain film-forming agent salts, activators, accelerators, pH adjusters and other additives for performance enhancement.[2,3] However, this article focuses on H_2ZrF_6 as the Zr-bearing component, although the influence of each additive in the conversion bath and their interactions on the subsequent performance is still not fully understood.[4,5]

While the chemistries of CCCs and PCCs have been studied in more detail using a variety of techniques throughout their use in the last century,[6,7] research on the aqueous chemistry of Zr was not sufficiently addressed, as evidenced by a limited number of studies.[8–10] In particular, spontaneous hydrolysis and condensation (*vide infra*) of Zr that slowly reaches an equilibrium state leads to the co-existence of various mononuclear and polynuclear species in the solution. This resulted in a relatively poor agreement between literature data regarding Zr-species and their stability constants.[8–10]

Brown et al.[8] gave a thorough thermochemical review of Zr and its compounds, including fluoride complexes. In an attempt to explain contradictory literature findings by establishing a single Zr-hydrolysis model, the authors included various monomeric and polymeric species, some of which had not been experimentally confirmed, namely $Zr_3(OH)_9{}^{3+}$, $Zr_4(OH)_{15}{}^{+}$ and $Zr_4(OH)_{16(aq)}$. This resulted in equilibrium constants of high uncertainty. Rai et al.[10] have recently developed a more comprehensive thermodynamic model by revising the available hydrolysis data for Zr and recalculating constants to be consistent with the more reliable data for its congener, Hf.[a]

For a complete elaboration of selection criteria in the Zr−OH system, readers are referred to Rai et al.[10] For Zr−F, values reported by Brown et al. are retained, with a full elaboration for selection criteria already given therein.[8]

Due to the reasons given above, we intend to review and display the state-of-the-art aqueous equilibria of Zr for Zr−OH and Zr−F systems with an emphasis on their hydrolysis behaviour. Although the manuscript may be overwhelmed with data, we attempted to compile all the information, which is, in our opinion, needed to explain the current reasons behind quite contradictory studies and provide the necessary background for future ones. Therefore, we hope this article will help researchers involved in conversion coatings to better understand the causes for current limitations and focus more on the solution chemistry behind Zr conversion bath constituents as it affects the final coatings' properties.

General Properties and Geometry of Zr Compounds

Zirconium (electronic configuration [Kr] $4d^2\ 5s^2$) is the 40th element belonging to the Group 4 of the Periodic table, with properties closely resembling titanium and hafnium. It is a lustrous silver–grey metal, exceptionally ductile, malleable and strong, yet lighter than steel (density 6.51 g cm^{-3}). Both Zr and its most common important derivative, crystalline ZrO_2 (zirconia), are resistant to most alkalis and acids (except HCl and H_2SO_4, and especially in the presence of F) as well as heat (melting point 1850 °C for Zr and 2710 °C for ZrO_2). In addition, ZrO_2 exceptional fracture toughness,chemical and heat resistance make it a suitable ceramic material, a thermal barrier coating, and a common diamond substitute.

Elemental Zr has a hexagonally close-packed crystal structure. In contrast, ZrO_2 has a monoclinic stable phase at room temperature,

[a]The intervening lanthanide contraction leads to nearly equal atomic and ionic radii for Zr and Hf (1.45 and 0.86 Å for Zr and Zr^{4+}; 1.44 and 0.85 Å for Hf and Hf^{4+}), making Hf a perfect chemical analogue to Zr.[11] Therefore, it is reasonable to expect hydrolysis constants for both elements to be similar in magnitude.[10]

*Electrochemical Society Member.
[z]E-mail: ingrid.milosev@ijs.si

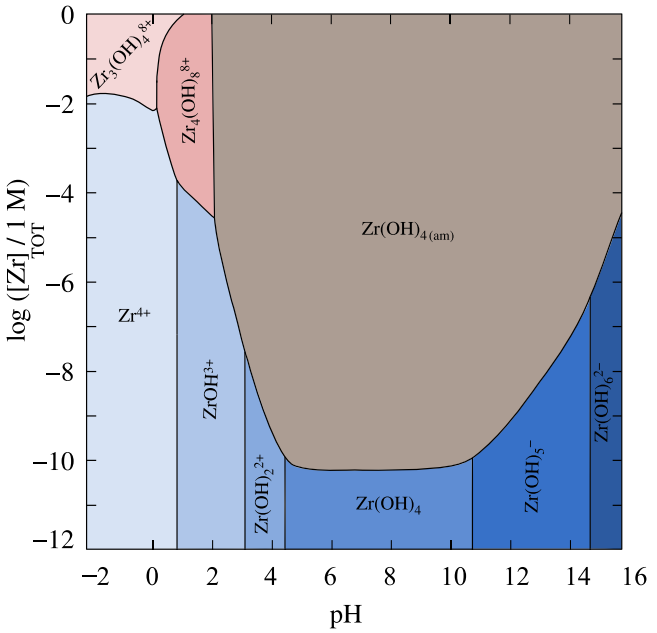

Figure 1. The updated predominance diagram for Zr(IV) species (with varying ionic strength in NaCl) at 25 °C.

which changes to tetragonal above 1100 °C, and cubic, fluorite-type above 2300 °C.[11–13] Like other transition metals, Zr forms a wide range of inorganic compounds and coordination complexes, most important being $ZrSiO_4$, ZrN, ZrC, ZrF_4, $ZrCl_4$, $ZrBr_4$ and ZrI_4.[11–13]

Due to its high charge-to-radius ratio and $4d^25s^2$ valence shell electron configuration, Zr is predominantly found in a tetravalent state in aqueous solutions. As is the case for all ions with charge $z \geqslant 4$, Zr aqueous chemistry is characterised by spontaneous and slow hydrolysis, yielding a highly acidic solution.[14,15]

Furthermore, having no partially filled shells leads to a lack of preferential geometry in Zr compounds. This, together with the low energy required for exchange from one geometry and coordination number to another, results in various Zr species in solid and liquid phases. In effect, Zr geometry is highly dependent on the nature of the current donor atoms (stoichiometry, size, and chelating ability) as well as vapour pressure, temperature, pH of the solution, etc.[11,16]

Experimental

Equilibria diagrams.—Zr chemical equilibria diagrams in this work were constructed using Spana (a Java equivalent to the former Medusa/Hydra software).[17,18] Spana's database contains equilibrium constants extrapolated to zero ionic strength (I = 0). This enables equilibria calculations at different pH and ionic strength values as well as ionic strength corrections arising from pH change and hydrolysis. For ionic strength corrections, either Davies equation, simplified Helgeson-Kirkham-Flowers (HKF), or Specific Ion Interaction Theory (SIT) can be used.[17,18]

Zr species with pertaining equilibrium constants and SIT parameters with Na^+ and Cl^- counterions were taken from Rai et al.[10] for Zr−OH calculations (Table I) and Brown et al.[8] for Zr−F calculations (Table II), respectively. Therefore, all equilibria herein are referred to aqueous NaCl solutions as a background electrolyte. The choice to employ SIT in this work was made following the recommendations by the Thermochemical Database (TDB) project of the Organisation for Economic Co-operation and Development—Nuclear Energy Agency (OECD–NEA TDB),[19,20] and was also used to derive equilibrium constants by Brown et al.[8] and Rai et al.[10] More details regarding SIT are given in the Supplementary information. To replicate H_2ZrF_6 stoichiometry in Spana, ZrF_6^{2-} was exchanged with Zr^{4+} as an input component, while F concentration was set to 0, assuming the resistance of ZrF_6^{2-} to hydrolysis.

Table I. Selected SIT ion-interaction parameters (ε) for modelling Zr–OH species at 25 °C.[8] and references within More details are presented in the Supplementary information.

Species	ε (kg mol^{-1})
H^+, Cl^-	0.12
Na^+, Cl^-	0.03
Na^+, OH^-	0.04
Zr^{4+}, Cl^-	0.33
$ZrOH^{3+}$, Cl^-	0.22
Na^+, $Zr(OH)_5^-$	0.03
Na^+, $Zr(OH)_6^{2-}$	0.07
$Zr_3(OH)_4^{8+}$, Cl^-	0.33
$Zr_4(OH)_8^{8+}$, Cl^-	1.37

Table II. Selected SIT ion-interaction parameters (ε) for modelling Zr–F species at 25 °C. More details are presented in the Supplementary information.

Species	ε (kg mol^{-1})	Reference
H^+, Cl^-	0.12	8
Na^+, Cl^-	0.03	8
Na^+, OH^-	0.04	8
Zr^{4+}, Cl^-	0.33	8
ZrF^{3+}, Cl^-	0.25	17,69
ZrF_2^{2+}, Cl^-	0.15	17,69
ZrF_3^+, Cl^-	0.05	17,69
Na^+,ZrF_5^-	−0.05	17,69
Na^+, ZrF_6^{2-}	−0.1	17,69

Computational method.—Ab initio calculations in the gas phase of the Zr tetramer, $Zr_4(OH)_8^{8+}$ (*vide infra*) were performed within the framework of Density Functional Theory (DFT) using an MN15 energy functional[21] as implemented within the Gaussian16 program package.[22] Zr tetramer structure shown herein was obtained from the structure proposed by Rai et al.[10] All atoms were described by the all-electron Def2TZVP basis set of Ahlrichs.[23] Standard geometry optimisation was performed to obtain a stable rearrangement of atoms and water molecules. An optimised structure was obtained using forces and the second derivative matrix (Hessian matrix) standard criteria as implemented in the Gaussian program package on the atoms, optimising the molecular structure to the local energy minimum. Molecular graphics were produced by the XCRYSDEN graphical package.[24] Figure 2 shows the Zr-tetramer structure with first-shell water molecules treated explicitly. To this end, structural and electronic properties based on molecular modelling were not investigated. DFT calculations in the scope of this article were performed for illustration purposes only and are not meant to obtain nor describe any new phenomena.

Results and Discussion

Hydrolysis and Zr–OH speciation.—Zr−OH predominance diagram is presented in Fig. 1, and the related reactions are presented in Table III. Please note that it does not make much sense to discuss the exact predominance regions for species present outside the range $2 > \text{pH} > 12$ due to uncertainty in activity coefficients[9]; however, the outer regions are kept for qualitative discussion.[b]

[b]Measuring the exact pH values lower than 2 and higher than 12 is complicated due to a significant change in water concentration, resulting in an incomplete strong acid dissociation and inconsistent activity coefficients. Hence, it would be more correct to represent the results regarding acid/alkali molality on the abscissa.[9,10,26] However, reaching these values is possible,[27,28] and are thus retained herein to demonstrate Zr behaviour in hyper-acidic and alkaline conditions, respectively. Although irrelevant for most of the environmental conditions, including conversion coatings, polymeric species serve here as a reminder for precipitation zirconia through a condensation process.

Table III. Selected cumulative stability and solubility constants ($\log_{10} K^0$) at I = 0 for modelling Zr–OH system at 25 °C.[8] and references within

Reaction / species	$\log_{10} K^0$
Mononuclear Zr hydrolysed species:	
$Zr^{4+} + 4H_2O \rightleftharpoons Zr(OH)_{4(am)} + 4H^+$	0.182
$Zr^{4+} + H_2O \rightleftharpoons ZrOH^{3+} + H^+$	0.32
$Zr^{4+} + 2H_2O \rightleftharpoons Zr(OH)_2^{2+} + 2H^+$	$\lesssim -2.304$
$Zr^{4+} + 4H_2O \rightleftharpoons Zr(OH)_{4(aq)} + 4H^+$	< -10.12
$Zr^{4+} + 5H_2O \rightleftharpoons Zr(OH)_5^- + 5H^+$	−19.66
$Zr^{4+} + 6H_2O \rightleftharpoons Zr(OH)_6^{2-} + 6H^+$	−33.29
Polynuclear Zr hydrolysed species:	
$3Zr^{4+} + 4H_2O \rightleftharpoons Zr_3(OH)_4^{8+} + 4H^+$	0.40
$4Zr^{4+} + 8H_2O \rightleftharpoons Zr_4(OH)_8^{8+} + 8H^+$	6.52

The constructed predominance diagram agrees with the general aqueous chemistry of Zr. Pure/free aqua ion Zr^{4+}, i.e. $[Zr(OH_2)_8^{4+}]$ practically does not exist except in hyper–acidic solutions[c] (pH < 0.5), resulting in quite an acidic onset of hydrolysis and precipitation (pH ~2 − 4).[8,9,11,30] $ZrOH^{3+}$ stands out as the most important mononuclear species followed by a less important $Zr(OH)_2^{2+}$,[10] both conferring to the previously observed existence of monomeric species at concentrations lower than 10^{-4} M.[31]

As pH and concentration increase, the formation of polynuclear species through hydrolysis and condensation proceeds continuously via charge compensation.[32] So far, Zr polymerisation paths starting from monomers, dimers, tetramers to octamers,[32] up to dodecamers have been suggested.[33] The polymerisation was found to be highly dependent on solution starting conditions, especially concentration, ageing, pH, and the presence of complexing agents.[32–35]

With many possible co-existing polymeric species, the diagram in Fig. 1 contains predominance areas only for $Zr_3(OH)_4^{8+}$ and $Zr_4(OH)_8^{8+}$,[d] to depict the existence of Zr-polymeric species above 10^{-4} M, aligned with previous findings.[34] Furthermore, in this article, a special focus was given to $Zr_4(OH)_8^{8+}$, as this species has been found with varying prevalence in most Zr-solution-based studies (*vide infra*).[10,16,32–46]

At the pH ~2 − 4, Zr precipitates in the form of an amorphous hydroxide, often referred to as "hydrated zirconia," $Zr(OH)_{4(s)/(am)}$.[e] Its stability extends over a large concentration range starting from 10^{-10} M, and a broad pH range from 2 to 16.[10] Zr, along with all highly charged tetravalent ions of *d*–block elements, acts as a strong acid, polarising both aqua and hydroxo ligands. Hence, formed amorphous hydroxide is unstable and undergoes spontaneous dehydration resulting in more or less hydrated oxyhydroxide of ill-defined composition, most correctly denoted as $ZrO_{2-x}(OH)_{2x}{,}yH_2O$.[14] However, in the literature, the Zr amorphous hydroxide phase is usually represented as either hydrous oxide $ZrO_2{\cdot}2H_{2O(s)}$, hydroxide $Zr(OH)_{4(s)/(am)}$ or zirconia amorphous oxide $ZrO_{2(am)}$.[2,12,30] In this article, we represent it as $Zr(OH)_{4(am)}$. Finally, in hyper-alkaline conditions, Zr hydroxylation yields anionic species $Zr(OH)_5^-$ and $Zr(OH)_6^{2-}$ with concentrations from 10^{-10} to 10^{-5} M.[f]

Taking hydrolysis strictly as a reaction with water, a general hydrolysis model for mononuclear and polynuclear Zr-species can be presented as reaction (2)[14]:

$$Zr(H_2O)_N^{4+} + qH_2O \rightleftharpoons Zr(OH)_q(H_2O)_{N-q}^{(4-q)+} + qH^+ \qquad [2]$$

For the sake of simplicity, aqua ligands in Zr hydroxoaqua complexes contained in the first hydration sphere are left out in this article.[g] This gives a simplified reaction (3)[8]:

$$mZr^{4+} + qH_2O \rightleftharpoons Zr_m(OH)_q^{(4m-q)+} + qH^+ \qquad [3]$$

It can be inferred that the free aqua $[Zr]^{4+}$ ion spontaneously hydrolyses, forming a monomer $[Zr(OH)]^{3+}$, which in turn olates to the cyclic tetramer $[Zr_4(OH)_8]^{8+}$ and possibly, even higher polynuclear forms. The degree of Zr polymerisation through hydrolysis increases with pH, and polynuclear species begin to predominate only at higher Zr concentrations (>10^{-4} M) [34], with the tetramer $Zr_4(OH)_8^{8+}$ being of particular interest and a common denominator in all Zr-solution based studies.[9,10,16,32–46]

The tetramer, $Zr_4(OH)_8^{8+}$.—The tetramer, $Zr_4(OH)_8^{8+}$ (more precisely, $[Zr_4(OH)_8(H_2O)_{16}]^{8+}$) obtains an eight-fold coordination, where four Zr atoms occupy corners of a distorted square linked along each edge by two bridging hydroxo groups (Fig. 2), thus exhibiting antiprismatic geometry.[14,51]

$Zr_4(OH)_8^{8+}$ has been detected in both liquid and solid states,[52,53] probably due to kinetic stability caused by symmetry and cyclisation.[16,32,43] However, ZrO_8, with a highly disordered lattice, has also been proposed.[49] Short-distance ordering, applicable to amorphous phases, is expected to significantly differ in the case of Zr due to its variability in geometry and coordination, thus disabling the establishment of a general precipitation model.[54–58] Nevertheless, assuming the existence of a generic link between the aqueous species and the formed solid, $Zr_4(OH)_8^{8+}$ can be considered the representative of all other polynuclear species and a fundamental building block of the solid phase (amorphous and crystalline). With the knowledge so far, Zr precipitates are formed from $Zr_4(OH)_8^{8+}$ either via electrostatic stacking or further change of geometry (see later Fig. 6).[32,44,49]

Updated E–pH diagram for Zr.—The original $E-$pH (Pourbaix) diagram for Zr is presented in Fig. 3. Zr has a very negative reduction potential, disabling production from aqueous solutions by electrolysis.[30] This makes the Pourbaix diagram of Zr just an inset from its general predominance diagrams at specific concentrations, more precisely 10^{-6}, 10^{-4}, and 10^{-2} M.

The original Pourbaix diagram contained Zr^{4+} cation in highly acidic solutions, hydrolysing to a zirconyl ion, ZrO^{2+}, in the pH range ~2 − 4. As such, ZrO^{2+} was used to represent all other mono − and polynuclear aqueous species.[30] The stable solid compound was represented as hydrated zirconium(IV) oxide, $ZrO_2 \cdot 2H_2O_{(s)}$, extending through a broad pH ~2 − 13. At pH > 13, Zr was presented to dissolve as zirconate ion, $HZrO_3^-$.

[c] In the literature, we have occasionally noticed incorrect records when conversion mechanisms were described using Zr^{4+} ion. This is incorrect since Zr^{4+} is stable only at pH levels lower than usually used in conversion baths. A brief but thorough discussion on correct inorganic chemistry nomenclature with emphasis on records for charge and oxidation states for various types of ions has been given recently.[29]

[d] Rai et al. [10] demonstrated that equilibrium constants values for the trimer ($Zr_3(OH)_4^{8+}$) and tetramer ($Zr_4(OH)_8^{8+}$) were significantly overestimated in Brown et al.[8] due to highly uncertain ion–interaction parameter values, making them irrelevant in a very extensive H^+ concentration range (10^{-1}–$10^{-15.4}$ mol kg^{-1}). However, values from Brown et al.[8] for the aforementioned polymers are retained in the light of describing further polymerisation paths. Indeed, $Zr_4(OH)_8^{8+}$ is the most experimentally studied and structurally confirmed Zr aqueous species. However, a recent Car–Parrinello molecular dynamics (CPMD) study has shown that trimer, although present here, may be a transient species rather than an essential component from which the tetramer is formed.[25].

[e] Fresh hydroxides are almost exclusively amorphous, which is in addition enhanced with increasing metal ion valency.[47] Kobayashi et al. speculated that room temperature precipitation of fresh $Zr(OH)_{4(am)}$ occurs via nanometric primary particles generating from weak electrostatic stacking of several $[Zr_2(OH)_4(H_2O)_8]^{4+}$ and $[Zr_4(OH)_8(H_2O)_{16}]^{8+}$.[44] These aggregated primary particles are randomly oriented and unhomogeniously dispersed. Tetramers have also been demonstrated to self–organize into cylindrical shapes, depending on pH and Zr precursor content.[48] On the other hand, ageing or refluxing Zr-solutions for extended periods leads to conversion from amorphous to more stable cubic or monoclinic crystalline hydrous zirconias, having intrinsically much lower values of solubility constants, i.e. being far less soluble.[35]

[f] Zirconate ion can be noted either as $HZrO_3^-$, ZrO_3^{2-} or $Zr(OH)_6^{2-}$, due to current inability to distinguish between them in solution-based solubility studies.[9] The latter is preserved here along with its equilibrium parameters from Rai et al.[10]

[g] The second hydration sphere was not even considered, as its identification is generally impeded by a rapid exchange with molecules in the bulk.[14,43,49,50]

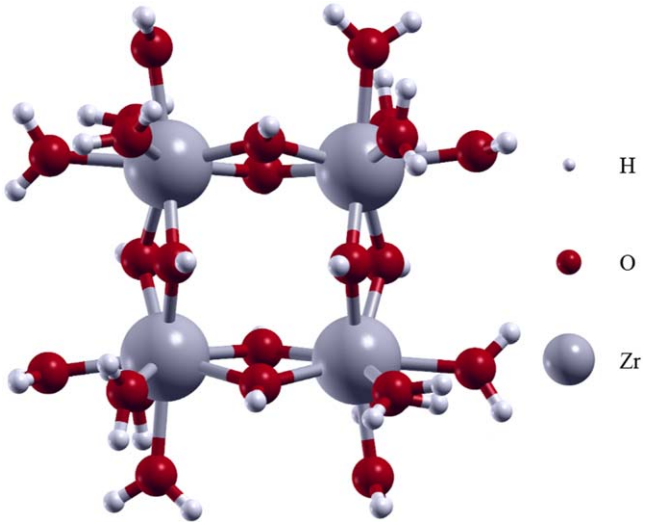

Figure 2. The optimised geometry of Zr tetramer, $Zr_4(OH)_8^{8+}$, calculated using the DFT method. (Courtesy of Matjaž Dlouhy from the Jožef Stefan Institute).

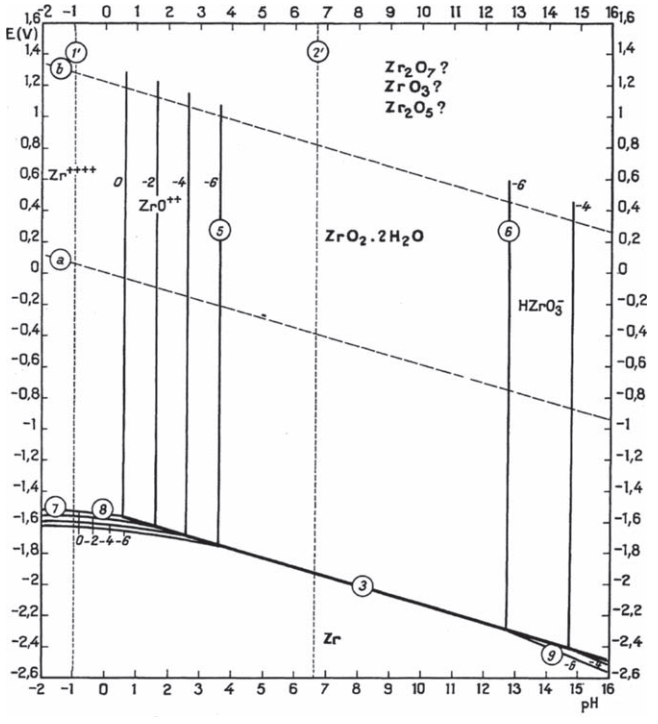

Figure 3. The original $E-$pH Pourbaix Zr–H_2O diagram at 25 °C.[30] *Reprinted from the book "Atlas of Electrochemical Equilibria in Aqueous Solutions" by Marcel Pourbaix, NACE, Cebelcor (Houston, Brussels), 1974, publisher National Association of Corrosion Engineers, with permission from AMPP Global Center, Inc.*

The updated Pourbaix diagram (Fig. 4) was constructed in Spana based on equilibrium data in Table III. Details for construction are given in the Supplementary information.

The main difference between the original and an updated diagram reflects in the choice of hydrolysed species. Since ZrO^{2+} existence had been conclusively disproven in both the aqueous and solid states,[52,53,59] we chose to depict mononuclear species with $ZrOH^{3+}$, and polynuclear with $Zr_4(OH)_8^{8+}$, respectively. Although the polynuclear Zr species should be excluded from the diagram by default, as they are not in equilibrium, $Zr_4(OH)_8^{8+}$ is used to establish the transition from

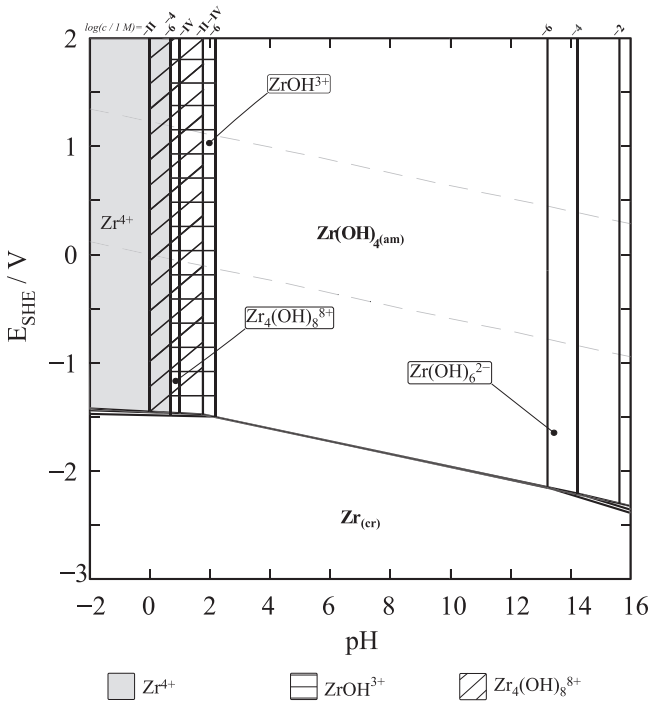

Figure 4. The updated $E-$pH Pourbaix Zr–H_2O diagram (with varying ionic strength in NaCl) at 25 °C. Callouts are added to point to the species. For easier reading, a legend is given below due to overlapping regions of monomeric and tetrameric species. In addition, the Roman numerals on top of the diagram indicate concentrations at which Zr tetramer exists. For all other species, the concentrations are given in Arabic numerals.

mononuclear to polynuclear species at Zr concentration $>10^{-4}$ M.[34] In this way, the thermodynamic stability of $Zr_4(OH)_8^{8+}$ was deliberately exchanged for its kinetic stability (*vide supra*).

In the end, both diagrams still share the similarity of the passive region from pH ~2 to 13, with a stable solid compound denoted here as $Zr(OH)_{4(am)}$ and zirconate ion as $Zr(OH)_6^{2-}$.[f] The existence of Zr compounds with different valencies or forms is not considered.[h]

Looking from ZrCCs perspective, the absence of soluble Zr species of higher valency above the $Zr(OH)_4$ region excludes the possibility of self-healing for Zr, in contrast to Cr. However, Zr non–toxicity and environmental friendliness, along with a much wider passivity region compared to metallic substrates on which ZrCCs are applied (steel, galvanised steel, aluminium and its alloys),[60–62] make it an attractive replacement, especially in terms of developing multi-metal coatings.

Zr–F speciation, hydrolysis and influence of F in the conversion bath.—Following the Hard and Soft Acids and Bases (HSAB) principle,[63] Zr−F complexes are quite stable fluoro-complexes,[64,65] with complexation proceeding up to ZrF_6^{2-}, according to the reaction (4)[8]:

$$Zr^{4+} + qF^- \rightleftharpoons ZrF_q^{4-q} \qquad [4]$$

It is thus not surprising that fluoride ions had been frequently added in Zr-containing solutions to prevent the early onset of hydrolysis,[66] a feature that was later used to facilitate the development of Zr conversion coatings. If all other Zr salts were used, dissolution in concentrated acids would be required. In contrast, this matter was solved all at once by introducing ZrF_6^{2-} anions that retain Zr solvated in the form of a fluoride complex.[67,68] Nowadays, ZrCC

[h]The existence of Zr aqueous compounds with a valency different than 4 that could theoretically occur in its oxide derivatives, especially at higher potentials, is unlikely. In addition, ZrH_2, due to its extreme stability, should eclipse the field of Zr. However, we opted to follow Pourbaix's practice and show elementary state of the metal in relation to its corrosion products.[30]

Table IV. Selected cumulative stability constants ($\log_{10}\beta^0$) at $I = 0$ for modelling Zr–F system at 25 °C.[8]

Reaction / species	$\log_{10}\beta^0$
$Zr^{4+} + F^- \rightleftharpoons ZrF^{3+}$	10.12
$Zr^{4+} + 2F^- \rightleftharpoons ZrF_2^{2+}$	18.55
$Zr^{4+} + 3F^- \rightleftharpoons ZrF_3^{+}$	24.72
$Zr^{4+} + 4F^- \rightleftharpoons ZrF_4$	30.11
$Zr^{4+} + 5F^- \rightleftharpoons ZrF_5^-$	34.60
$Zr^{4+} + 6F^- \rightleftharpoons ZrF_6^{2-}$	38.11

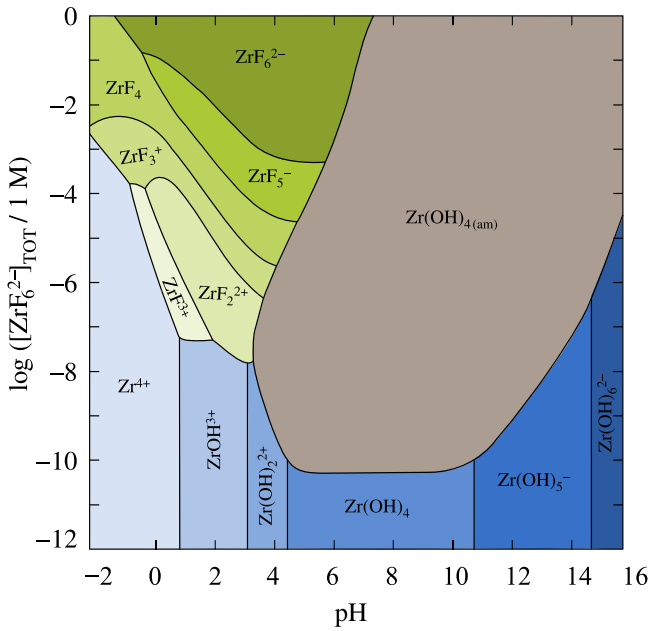

Figure 5. The updated predominance diagram for Zr−F species (with varying ionic strength in NaCl) at 25 °C.

baths have hexafluorozirconate commonly added as a salt or acid, i.e. K_2ZrF_6 or H_2ZrF_6.[2]

Table IV contains equilibrium constants for the Zr−F complexes from Brown et al.[8] with calculated SIT parameters (Table II)[17,69] from which a Zr−F predominance diagram in Fig. 5 was constructed. It can be seen that stable Zr−F complexation in H_2ZrF_6, occurring at concentrations above $\sim 10^{-4}$ M, raises the precipitation pH (compare Figs. 1 and 5), which is further increased with H_2ZrF_6 concentration. However, performing conversion with high H_2ZrF_6 concentrations would lead to insufficient pH rise, a decrease in the coating's Zr content,[70,71] and an increase in F^- content. Consequently, ZrCCs are most commonly produced in the pH range 4 – 4.6 [2 and refs therein] and concentrations expressed as Zr ion 10 – 30 wt%.[72–75]

The little reference given to ZrF_6^{2-} solutions are summarised as follows: ZrF_6^{2-} was shown to be the only mononuclear species present in solutions containing ZrF_5^- and ZrF_7^{3-} ions, thus suggesting its high stability.[76] After adding alkali to aqueous solutions of ZrF_6^{2-}, only ZrF_6^{2-} and F^- ions were detected, with no additional hydrolysis species. The remainder precipitated rapidly as colloidal polynuclear fluorohydroxocomplexes (PFHCs) with a Zr:F ratio of 1:3, thus suggesting high lability of ZrF_6^{2-}.[77] In another study, it was also shown that Zr−F does not undergo complete hydrolysis,[78] which supports general X-ray photoelectron spectroscopy (XPS) findings on ZrCCs composition as a mixture of primary ZrO_2 with lower amounts of ZrF_4, oxyhydroxide and/or oxyfluoride in ZrCCs.[70,79]

As we can see, the speciality of ZrF_6^{2-} that enabled the development of ZrCCs seems to lie in its simultaneous stability and lability (please note that the lability is a kinetic parameter and indicates how fast a metal ligand is exchanged, whereas stability is a thermodynamic parameter, defined by the formation constant).[80] Nevertheless, hydrolysis of ZrF_6^{2-} is complicated by the existence of F^- as a complexing agent in the inner ligand sphere. For comparison, Cl^- ions occupy only the outer ligand sphere during complexation with Zr and are more prone to rapid exchange with solution molecules than F^-.[53] However, F^- is more electronegative than water; thus, the nature of the Zr−F bond is more ionic and more susceptible to ionic dissociation. This is further enhanced by a high exchange rate with OH^- ion due to similarities in ionic radii.[81] Therefore, hydrolysis of H_2ZrF_6 can be best described as an isomorphic substitution of F^- with OH^- (*vide infra*), as shown in the case of antimony and silicon fluoride complexes.[82,83]

As ZrF_6^{2-} ions have been shown to be significantly less aggressive than free F^- in terms of oxide film thinning, their primary role in ZrCC baths appears to be surface activation via a significant increase in wettability.[4] In contrast, the synergistic action of acid and free F^- (added in the formulation or recovered from the reaction) leads to the thinning of native surface film, hence enabling electron tunnelling, the latter being crucial for Al and its alloys.[4] However, on Mg alloy, it has been reported that free F^- suppresses Zr-film formation by interfering with the reaction of Zr with OH^- liberated by cathodic reaction rather than by substituting the existing OH^- of the surface layer.[70] High hydrophilicity and acidity make ZrCCs ideal for improving subsequent adhesion but not corrosion protection properties at the same time.[84]

Sol-gel and electrochemical perspectives of the formation of Zr (hydr)oxide formed by conversion.—Reaction (1) represents a simplified precipitation mechanism of Zr oxide in ZrCCs. In the hitherto published literature, much of the emphasis on the precipitation of Zr oxide in ZrCCs has been given to the electrochemical properties of the substrate/coating system only. In this process, hydroxylation is induced by the cathodic reactions and consequent rise in pH. However, the progress of the coating formation and the overall process is indeed based on sol-gel chemistry. Therefore, understanding the coatings' formation from both sol-gel and electrochemical perspectives is a prerequisite for improving their overall performance.

Self-hydrolysis and thermally-induced hydrolysis of Zr, both relatively slow processes, lead to homogeneous and higher-ordered structures.[14,35,51] On the other hand, accelerating hydrolysis through forced hydrolysis by adding base results in disordered structures. In particular, a diffusion-controlled hydroxylation by alkalinisation (essentially present at the cathodic sites of a heterogeneous alloy surface during hydrogen and oxygen reduction in the course of ZrCCs formation) is exceptionally rapid,[85] with overlapping nucleation and growth processes. In other words, rapid base addition leads to the formation of local pH gradients, i.e. random distribution of hydroxyls on the tetramer. Consequently, polymerisation occurs in many directions simultaneously, as there is not enough time to form an ordered array of tetramers. As a result, the obtained product is an amorphous gel rather than a crystal.[14,35,51] The two described scenarios are presented in Fig. 6 based on the pioneering work by Clearfield.[51] It can be observed that the tetrameric network expands as free water molecules at the edges are allowed to hydrolyse continuously.[35,51] Further polymerisation and/or stacking of tetrameric units[32,44,49] leads to precipitation of the solid phase, as the conditions allowing the nucleophilic substitution on the growing oligomer are no longer present.[14]

It should be noted that a higher electrical charge, as in the case of $Zr_4(OH)_8^{8+}$ tetramer, limits the formation of condensed species, whereas neutral precursors can condense freely to solid (virtually infinitely). Precipitation can occur over a wide range of acidity, frequently much outside the predominance zone of a noncharged metal species. In the case of Zr, this might occur via species such as

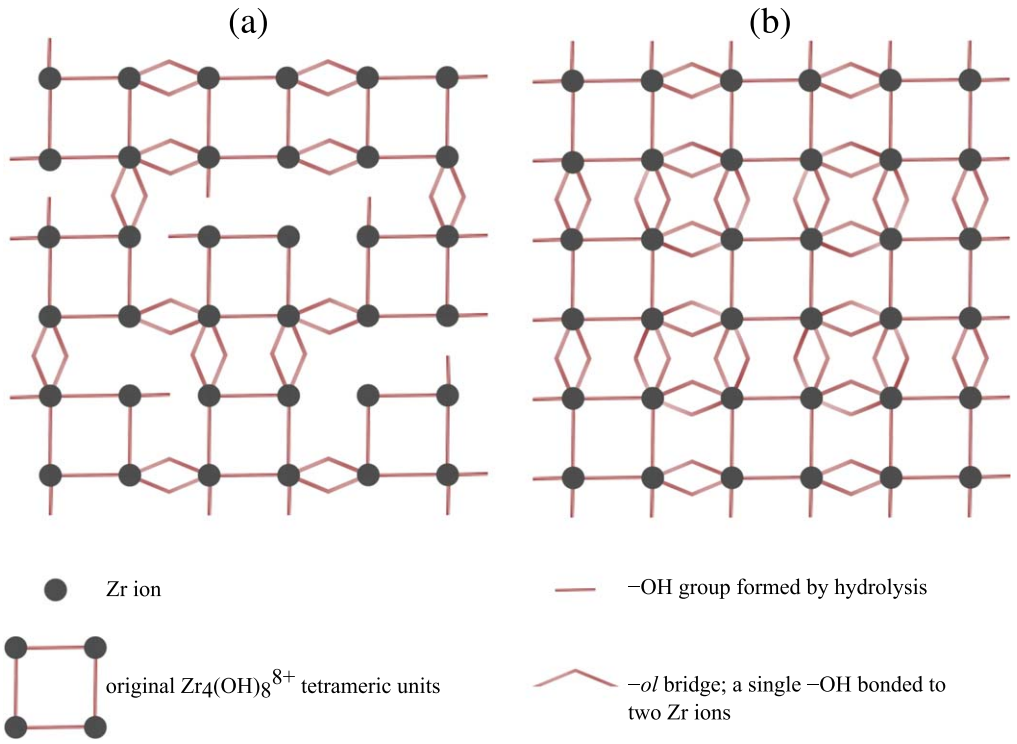

Figure 6. Schematic illustration of two–dimensional Zr tetramer condensation. (a) Randomly formed polymer obtained by fast hydrolysis, such as base addition (including ZrCCs). (b) Ordered sheet polymer produced by slow hydrolysis, such as heating. Figure modified from Clearfield.[51]

$Zr(OH)_{4(aq)}$ or tetrameric $Zr(OH)_{16(aq)}$, for the latter of which no solid evidence exists.[14] However, it was also found that Zr precipitation can occur via species of lower charge[i] than $Zr_4(OH)_8^{8+}$.[32]

After the layer of a condensed sol containing polynuclear particles has been created, the resulting gel's high permeability, ionic conductivity, open structure, and high water retention allow for continued gelation and film growth through alkalisation and nucleation via formed colloidal particles.[81,86]

In the case of Zr, olation, reaction (5), can be followed by oxolation, reaction (6), of terminal OH^- groups[14]:

$$M - OH + M - OH_2 \rightarrow M - OH - M + H_2O \quad [5]$$

$$M - OH + OH - M \rightarrow M - O - M + H_2O \quad [6]$$

The rate constant of oxolation of Zr is much slower (by two orders of magnitude) than olation.[87] Nevertheless, the tendency toward oxolation increases with an increase in pH,[57] so a sufficient rise during conversion could lead to oxolation.

Conventional sol-gel synthesis, also applied in several examples on zirconium conversion coatings,[88–91] most often includes alkoxy precursors, enabling fine-tuning of hydrolytic rate and path through the ratio of alkoxy precursors to water as well as the addition of various complexing agents.[81] This leads to separated sol and gel stages. In contrast, in ZrCC, the precipitation based on H_2ZrF_6 sol and gel stages occur consecutively in the vicinity of the metal surface, thus not leaving much space for control of distinctive stages or reaction rates. Therefore, a better understanding of the aqueous thermodynamics of Zr should be the first step in elucidating the control of Zr hydrolytic rate and path.

From an electrochemical perspective, anodic areas of the metal surface matrix undergo oxidation, accompanied by hydrogen and oxygen reduction at cathodic areas (such as intermetallic particles (IMPs) and grain boundaries), eventually leading to surface alkalisation and precipitation. Thus, ZrCC preferentially deposits at cathodic areas and grows in the lateral direction until full metal coverage. As a result, ZrCCs have an inconsistent thickness, ranging between 10 and 80 nm, which is significantly lower and could be disadvantageous compared to its ancestor technologies.[2]

We can try applying the above-described sol-gel chemistry of Zr −OH to Zr−F as follows:isomorphic substitution of F^- with OH^- during hydroxylation of ZrF_6^{2-} results in the formation of aquahydroxo/aquafluorohydroxo complexes. Hydroxo ligand, in turn, acts as a nucleophilic entering group inducing substitution of an aqua ligand in another complex. Condensation initiated by alkalisation shouldinclude discrete polycationic species starting from monomers, proceeding with dimers and, most probably, ending with some form of tetramers. More substantial evidence for this was given in older studies on thermo- and alkali-hydrolysis of Zr oxyfluorides, at least in the crystalline phase.[92–94] Figure 6a can therefore be used for describing ZrCC precipitation as well. Nevertheless, it is hard to postulate any exact species involved in the hydrolysis and precipitation of H_2ZrF_6 solutions, as the polymerisation path significantly depends on starting solution conditions, in this case, F^- as a complexing agent.[35]

The conversion process should occur until the exhaustion of the conversion agent (Zr-bearing components) and suppression of local cathodic activity at the metal surface, making the process self-limiting.[73,95,96] Hence, studies of conversion coating processes should be directed toward managing the electrochemical aspects, especially those that would allow control of pH increase during conversion (e.g. through the control of density and electroactivity of IMPs,[97] application of electro-assisted deposition,[98] etc.), as well as its sol-gel nature, as already elaborated for Cr conversion coatings.[15,86,99,100]

As seen from reaction (1), the ZrCC process is accompanied by the regeneration of the hydrofluoric acid. Determining total and free-fluoride content is crucial to establish equilibrium between the former and hydrolysis reaction, as too high concentration leads to excess metal dissolution, while too low concentration leads to insufficient

[i]While there is no significant change in charge as pH rises, Walther *et al.* demonstrated that a decrease of tetrameric species concentration with an increase of higher polynuclear species (pentamers, octamers) concentration, as well as a decrease in their mean charge value to 2 near the solubility limit, supports precipitation of $Zr(OH)_{4(am)}$ by larger, yet less charged species than $Zr_4(OH)_8^{8+}$.[32]

coating formation. In addition, F^- retained in the coating is detrimental to the underlying substrate.[2,84] Nevertheless, hydrated zirconia has ionic exchange properties, and the amount of retained anions in the precipitate decreases with an increase in the final precipitation pH.[35,37] In the case of F^-, due to the aforementioned high lability, proper rinsing with clean deionised water can significantly minimise F^- content.[72,84,101] Moreover, the amount of F^- in commercial ZrCCs is minimised by blending with other additives, such as Cu, Zn, Mn, Co, alkaline Earth metal ions[102] and H_3BO_3.[103]

To sum up, nowadays, F^- is an essential component of ZrCC baths yet detrimental to the underlying substrate, which requires thorough studies on Zr−OH and ZrF_6^{2-} solutions. However, the determination of solvated ion structures requires various scattering, absorption and resonance spectroscopy methods combined with computer simulations.[104] Most of those methods are not readily available or require synchrotron radiation, which, along with fast hydrolysis and exchange of Zr geometry and coordination, makes the deduction of exact polymerisation paths and species involved in the process still challenging. Although some of the methods have been successfully employed for Zr–OH systems without F,[32,43–45,48,49,105] to the best of our knowledge, no absorption or scattering studies were explicitly conducted on Zr−F complexes, which would considerably help to reveal ZrCC coating formation.

Conclusions

Limited knowledge of ZrCC chemistry directly results from limited knowledge of Zr aqueous chemistry. The high tendency of zirconium to hydrolyse, along with a rapid exchange of geometry, coordination, and sensitivity to solution composition, significantly impedes the study of composition and geometry of Zr compounds. The primary function of hexafluorozirconate is to provide an activated metal surface while also adjusting the pH from severely acidic to that acceptable for conversion. In this study, revised predominance areas for Zr−OH and Zr−F aqueous speciation concerning Zr amorphous phase were established as a foundation for describing the ZrCC formation mechanism. The tetramer, $Zr_4(OH)_8^{8+}$, was used to represent all other polynuclear species and a fundamental building block of the solid phase. Revised Zr equilibria were the basis for the updated E−pH (Pourbaix) diagram, comprising $ZrOH^{3+}$ and $Zr_4(OH)_8^{8+}$ instead of formerly employed ZrO^{2+}.

We believe this study can serve as a starting point for future extensions to other additives utilised in ZrCC baths, as well as the elucidation of their effects and interactions. This could, at the very least, direct field researchers to focus their research on the final coating and the solution chemistry behind Zr conversion bath components. The electrochemical nature of the conversion process is reflected in its initiation; however, the core of the process is based on hydrolysis and condensation. Thus, future efforts to identify ways to control electrochemical and sol-gel chemistry could be critical in increasing the overall performance of ZrCCs.

Acknowledgments

This research was funded by Slovenian Research Agency (research core funding grant P2–0393 and project PR–09806). The authors would like to extend their heartfelt thanks to Dr Ignasi Puigdomènech of Swedish Nuclear Fuel and Waste Management Co. (SKB) for fruitful discussions and generous expert advice on constructing diagrams using Spana. The authors also express their gratitude to Mr Matjaž Dlouhy of the Department of Physical and Organic Chemistry for performing the DFT calculations and preparing the Zr tetramer structure (Fig. 2), as well as to Prof. Anton Kokalj for insightful discussions.

ORCID

Ana Kraš https://orcid.org/0000-0002-3499-0853
Ingrid Milošev https://orcid.org/0000-0002-7633-9954

References

1. *CRC Handbook of Chemistry and Physics*D. Lide (ed.), (Boca Raton, FL, CRC Press) 84th ed. (2004).
2. I. Milošev and G. S. Frankel, *J. Electrochem. Soc.*, **165**, C127 (2018).
3. K. Ogle and R. G. Buchheit, "Conversion Coatings." *Encyclopedia of Electrochemistry, Corrosion and Oxide Films*, ed. A. J. Bard and M. Stratmann (Weinheim, Germany, Wiley-VCH) Vol. 4, p. 460 (2003).
4. D. Chidambaram, C. R. Clayton, and G. P. Halada, *Electrochim. Acta*, **51**, 2862 (2006).
5. J. Han, D. Thierry, and K. Ogle, *Surf. Coat. Technol.*, **402**, 126236 (2020).
6. T. S. N. S. Narayanan, *Rev. Adv. Mater. Sci.*, **9**, 130 (2005).
7. M. Doerre, L. Hibbitts, G. Patrick, and N. K. Akafuah, *Coatings*, **8**, 405 (2018).
8. P. L. Brown, E. Curti, and B. Grambow, *Chemical Thermodynamics of Zirconium, OECD Nuclear Energy Agency* (Amsterdam, The Netherlands, Elsevier) 1st ed. (2005).
9. P. L. Brown and C. Ekberg, *Hydrolysis of Metal Ions* (Wiley-VCH, Weinheim, Germany) (2016).
10. D. Rai, A. Kitamura, M. Altmaier, K. M. Rosso, T. Sasaki, and T. Kobayashi, *J. Solution Chem.*, **47**, 855 (2018).
11. *Advanced Inorganic Chemistry*F. A. Cotton, G. Wilkinson, C. A. Murillo, and M. Bochmann (ed.), (New York, Wiley) 6th ed. (1999).
12. R. J. H. Clark, D. C. Bradley, and P. Thornton, *Comprehensive Inorganic Chemistry, Series Pergamon Texts in Inorganic Chemistry.*, ed. J. C. Bailar Jr, H J. Emeléius, R. Nyholm, and A. F. Trotman-Dickenson (Oxford, UK, Pergamon Press) p. 419 (1973).
13. G. D. Considine, *Van Nostrand's Encyclopedia of Chemistry* (New Jerseyk, Wiley) 5th ed. (2005).
14. J.-P. Jolivet, *Metal Oxide Nanostructures Chemistry: Synthesis from Aqueous Solutions* (New York, Oxford University Press) 2nd ed. (2019).
15. J. H. Osborne, *Prog. Org. Coat.*, **41**, 280 (2001).
16. T. E. Macdermott, *Coord. Chem. Rev.*, **11**, 1 (1973).
17. I. Puigdomènech, (2020), Spana https://sites.google.com/site/chemdiagr/home/java-versions.
18. I. Puigdomènech, E. Colàs, M. Grivé, I. Campos, and D. García, *MRS Online Proc. Libr.*, **1665**, 111 (2014).
19. https://oecd-nea.org/.
20. F. J. Mompeán and H. Wanner, *Radiochim. Acta*, **91**, 617 (2003).
21. H. S. Yu, X. He, S. L. Li, and D. G. Truhlar, *Chem. Sci.*, **7**, 5032 (2016).
22. M. J. Frisch et al., (2016), Gaussian 16, Revision C.01.
23. F. Weigend and R. Ahlrichs, *Phys. Chem. Chem. Phys.*, **7**, 3297 (2005).
24. A. Kokalj, *J. Mol. Graph. Model.*, **17**, 176 (1999).
25. N. Rao, M. N. Holerca, and V. Pophristic, *J. Chem. Theory Comput.*, **4**, 145 (2008).
26. I. Grenthe and I. Puigdomenech (ed.), "OECD Nuclear Energy Agency." *Modelling in Aquatic Chemistry* (OECD Publications, Paris) (1997).
27. K. F. Lim, *J. Chem. Educ.*, **83**, 1465 (2006).
28. R. G. Bates and A. K. Vijh, *Determination of pH: Theory and Practice* (New York, Wiley) 2nd ed. (1973).
29. D. K. Kozlica and I. Milošev, *CORROSION*, **77**, 696 (2021).
30. M. Pourbaix, *Atlas of Electrochemical Equilibria in Aqueous Solutions* (Houston (TX), Brussels, National Association of Corrosion Engineers) 2nd ed. (1974).
31. R. E. Connick and W. H. McVey, *J. Am. Chem. Soc.*, **71**, 3182 (1949).
32. C. Walther, J. Rothe, M. Fuss, S. Büchner, S. Koltsov, and T. Bergmann, *Anal. Bioanal. Chem.*, **388**, 409 (2007).
33. T. Sasaki, O. Nakaoka, R. Arakawa, T. Kobayashi, I. Takagi, and H. Moriyama, *J. Nucl.Sci. Technol.*, **47**, 1211 (2010).
34. R. E. Connick and W. H. Reas, *J. Am. Chem. Soc.*, **73**, 1171 (1951).
35. A. Clearfield, *J. Mater. Res.*, **5**, 161 (1990).
36. D. A. Zyuzin, E. M. Moroz, A. S. Ivanova, and A. N. Shmakov, *Crystallogr. Reports*, **48**, 413 (2003).
37. A. Clearfield, G. P. D. Serrette, and A. H. Khazi-Syed, *Catal. Today*, **20**, 295 (1994).
38. M. M. Kasprzak, A. Erxleben, and J. Ochocki, *RSC Adv.*, **5**, 45853 (2015).
39. T. Sasaki, T. Kobayashi, I. Takagi, and H. Moriyama, *J. Nucl. Sci. Technol.*, **45**, 735 (2008).
40. T. Kobayashi, D. Bach, M. Altmaier, T. Sasaki, and H. Moriyama, *Radiochim. Acta*, **101**, 645 (2013).
41. M. Altmaier, V. Neck, and T. Fanghänel, *Radiochim. Acta*, **96**, 541 (2008).
42. Y.-J. Hu, K. E. Knope, S. Skanthakumar, M. G. Kanatzidis, J. F. Mitchell, and L. Soderholm, *J. Am. Chem. Soc.*, **135**, 14240 (2013).
43. C. Hagfeldt, V. Kessler, and I. Persson, *Dalt. Trans.*, **14**, 2142 (2004).
44. T. Kobayashi, S. Nakajima, R. Motokawa, D. Matsumura, T. Saito, and T. Sasaki, *Langmuir*, **35**, 7995 (2019).
45. P. D. Southon, J. R. Bartlett, J. L. Woolfrey, and B. Ben-Nissan, *Chem. Mater.*, **14**, 4313 (2002).
46. C. Ekberg, G. Källvenius, Y. Albinsson, and P. L. Brown, *J. Solution Chem.*, **33**, 47 (2004).
47. "Section of analytical chemistry of the international union of pure and applied chemistry." *Solubility constants of metal oxides, metal hydroxides and metal hydroxide salts in aqueous solution.*W. Feitknecht and P. Schindler (ed.), (London, UK, Butterworths) p. 125 (1963).
48. A. Gossard, G. Toquer, S. Grandjean, and A. Grandjean, *J. Sol-Gel Sci. Technol.*, **71**, 571 (2014).
49. H.-R. Cho, C. Walther, J. Rothe, V. Neck, M. A. Denecke, K. Dardenne, and T. Fanghänel, *Anal. Bioanal. Chem.*, **383**, 28 (2005).

50. T. S. Hofer, A. K. H. Weiss, B. R. Randolf, and B. M. Rode, *Chem. Phys. Lett.*, **512**, 139 (2011).
51. A. Clearfield, *Rev. Pure Appl. Chem.*, **14**, 91 (1964).
52. A. Clearfield and P. A. Vaughan, *Acta Crystallogr.*, **9**, 555 (1956).
53. G. M. Muha and P. A. Vaughan, *J. Chem. Phys.*, **33**, 194 (1960).
54. M. J. D. Rushton, I. Ipatova, L. J. Evitts, W. E. Lee, and S. C. Middleburgh, *RSC Adv.*, **9**, 16320 (2019).
55. D. Vanderbilt, X. Zhao, and D. Ceresoli, *Thin Solid Films*, **486**, 125 (2005).
56. M. Durandurdu, *Philos. Mag.*, **97**, 1334 (2017).
57. M. Henry, J.-P. Jolivet, and J. Livage, *Chemistry, Spectroscopy and Applications of Sol-Gel Glasses, Structure and Bonding.*, ed. R. Reisfeld and C. K. JJørgensen (Berlin, Germany, Springer Berlin–Heidelberg) Vol. 77, p. 153 (1992).
58. J. Livage, K. Doi, and C. Mazieres, *J. Am. Ceram. Soc.*, **51**, 349 (1968).
59. A. S. Solovkin and Z. N. Tsvetkova, *Russ. Chem. Rev.*, **31**, 655 (1962).
60. P. D. Deck and D. W. Reichgott, *Met. Finish.*, **90**, 29 (1992).
61. N. W. Khun and G. S. Frankel, *CORROSION*, **71**, 277 (2015).
62. R. Mohammad Hosseini, A. A. Sarabi, H. E. Mohammadloo, and M. Sarayloo, *Surf. Coat. Technol.*, **258**, 437 (2014).
63. R. G. Pearson, *J. Am. Chem. Soc.*, **85**, 3533 (1963).
64. A. K. Babko, *Russ. J. Inorg. Chem.*, **4**, 485 (1959).
65. G. Goldstein, *Anal. Chem.*, **36**, 243 (1964).
66. R. M. Sawant, U. K. Thakur, and K. L. Ramakumar, *J. Solution Chem.*, **34**, 113 (2005).
67. C. E. Tomlinson, (1995), https://patents.google.com/patent/US5380374A/en.
68. B. Dunham, *Met. Finish.*, **110**, 18 (2012).
69. W. Hummel, *Ionic strength corrections and estimation of SIT ion interaction coefficients, Report PSI-TM-44-09-01* (Paul Scherrer Institut, Villigen, Switzerland) (2009).
70. S. Verdier, S. Delalande, N. van der Laak, J. Metson, and F. Dalard, *Surf. Interface Anal.*, **37**, 509 (2005).
71. S. Verdier, N. van der Laak, F. Dalard, J. Metson, and S. Delalande, *Surf. Coat. Technol.*, **200**, 2955 (2006).
72. Y. Guan, J.-G. G. Liu, and C.-W. Wei Yan, *Int. J. Electrochem. Sci.*, **6**, 4853 (2011).
73. H. E. Mohammadloo, A. A. Sarabi, R. Mohammad Hosseini, M. Sarayloo, H. Sameie, and R. Salimi, *Prog. Org. Coat.*, **77**, 322 (2014).
74. H. E. Mohammadloo and A. A. Sarabi, *Appl. Surf. Sci.*, **387**, 252 (2016).
75. L. Zhu, F. Yang, and N. Ding, *Surf. Coat. Technol.*, **201**, 7829 (2007).
76. L. Kolditz and A. Feltz, *Z. Anorg. Allg. Chem.*, **310**, 195 (1961).
77. M. A. Fedotov and A. V. Belyaev, *J. Struct. Chem.*, **52**, 69 (2011).
78. V. P. Tolstoi and B. Altangerel, *Russ. J. Gen. Chem.*, **76**, 1716 (2006).
79. M. M. Kim, B. Kapun, U. Tiringer, G. Šekularac, and I. Milošev, *Coatings*, **9**, 563 (2019).
80. *Inorganic Chemistry: Principles of Structure and Reactivity*J. E. Huheey, E. A. Keiter, R. L. Keiter, and O. K. Medhi (ed.), (New York, Harper Collins College Publishers) 4th ed. (1993).
81. C. J. Brinker and G. W. Scherer, *Sol-Gel Science: The Physics and Chemistry of Sol-Gel Processing* (Boston, Academic Press) 1st ed. (1990).
82. N. M. Laptash, E. V. Kovaleva, A. A. Mashkovskii, A. Y. Beloliptsev, and L. A. Zemnukhova, *J. Struct. Chem.*, **48**, 848 (2007).
83. C. E. Roberson and R. B. Barnes, *Chem. Geol.*, **21**, 239 (1978).
84. C. E. Tomlinson, (1999), https://patents.google.com/patent/US5952049A/en.
85. C. F. Baes and R. E. Mesmer, *The Hydrolysis of Cations* (New York, Wiley) (1976).
86. P. Campestrini, G. Goeminne, H. Terryn, J. Vereecken, and J. H. W. de Wit, *J. Electrochem. Soc.*, **151**, B59 (2004).
87. N. V. Nikolenko, V. G. Vereshchak, A. D. Grabchuk, and O. S. Ostrovskaya Dnepropetrovsk, *Zh. Fiz. Khim.*, **69**, 822 (1995).
88. S. K. Tiwari, M. Tripathi, and R. Singh, *Corros. Sci.*, **63**, 334 (2012).
89. I. Milošev, B. Kapun, P. Rodič, and J. Iskra, *J. Sol-Gel Sci. Technol.*, **74**, 447 (2015).
90. X. F. Yang, D. E. Tallman, V. J. Gelling, G. P. Bierwagen, L. S. Kasten, and J. Berg, *Surf. Coat. Technol.*, **140**, 44 (2001).
91. P. Rodič, S. Zanna, I. Milošev, and P. Marcus, *Front. Mater.*, **8**, 756447 (2021).
92. Y. A. Bushlaev, Y. E. Gorbunova, and M. P. Gustyakova, *Bull. Acad. Sci. USSR, Div. Chem. Sci.*, **11**, 177 (1962).
93. L. Kolditz and A. Feltz, *Z. Anorg. Allg. Chem.*, **310**, 204 (1961).
94. L. Kolditz and A. Feltz, *Z. Anorg. Allg. Chem.*, **310**, 217 (1961).
95. H. Eivaz Mohammadloo, A. A. Sarabi, A. A. Sabbagh Alvani, H. Sameie, and R. Salimi, *Surf. Coat. Technol.*, **206**, 4132 (2012).
96. T. Lostak, S. Krebs, A. Maljusch, T. Gothe, M. Giza, M. Kimpel, J. Flock, and S. Schulz, *Electrochim. Acta*, **112**, 14 (2013).
97. P. Campestrini, E. P. M. van Westing, and J. H. W. de Wit, *Electrochim. Acta*, **46**, 2631 (2001).
98. V. Bonamigo Moreira, A. Puiggalí-Jou, E. Jiménez-Piqué, C. Alemán, A. Meneguzzi, and E. Armelin, *Materials (Basel).*, **14**, 1043 (2021).
99. N. V. Mandich, *Plat. Surf. Finish.*, **84**, 108 (1997).
100. W. Zhang, B. Hurley, and R. G. Buchheit, *J. Electrochem. Soc.*, **149**, B357 (2002).
101. E. Ramanathan and S. Balasubramanian, *Prog. Org. Coat.*, **93**, 68 (2016).
102. M. Matsukawa, K. Makino, and T. Shimakura, (2004), https://patents.google.com/patent/US20040187967A1/en.
103. S. Le Manchet, D. Verchère, and J. Landoulsi, *Thin Solid Films*, **520**, 2009 (2012).
104. H. Ohtaki and T. Radnai, *Chem. Rev.*, **93**, 1157 (1993).
105. M. Savastano, C. Bazzicalupi, G. Ferraro, E. Fratini, P. Gratteri, and A. Bianchi, *Molecules*, **24**, 2098 (2019).